



SIMULATION OF AVIONICS ELECTROMAGNETIC SHIELDING EFFECTIVENESS BASED ON MODAL MOM

YAJUN XU

Civil Aviation Flight University of China, Aviation Engineering Institute, Civil Aviation Flight University of China, Guanghan Sichuan, China (618307), 086-0838-5182655

E-mail: genius98@126.com

ABSTRACT

In this paper, an efficient technique based on modal method of moments (MoM) is presented, the influence of apertures' shape and calculation point of SE on electromagnetic shielding effectiveness has been studied. A very good agreement among the simulation results of the proposed technique, results available in the literature and experimental results is observed. The results of the present analysis show that electric field SE is seriously affected by calculation points and aperture shape. These useful results gained in this paper have important practical significance to improving the electric field shielding effectiveness of shielding cavity.

Keywords: *Rectangular Enclosure, Apertures, SE, Mom, Green's Function*

1. INTRODUCTION

In the past most aircraft used a series of cables, chains, cranks, and mechanical mechanisms to operate the systems which gave the aircraft its ability to fly. With the advent of the transistor many mechanical devices have been replaced or augmented with electronic circuits. Electronic circuits have increasingly been designed and used for flight critical aircraft control systems, due to their ability to accurately control complex functions and increase reliability. Electronic circuits, however, not only respond to their internal electrical signal flow, but may respond to any input which can couple into the wire bundles, wires, IC leads, and electrical junctions. The Electromagnetic Environment (EME) is one of these inputs that by its nature has access to all these electronic circuits and may result in disabling effects called Electromagnetic Interference (EMI). The aircraft skin and structure have also evolved. The classic aircraft is made of aluminum and titanium structure with an aluminum skin. Modern technology and the desire to develop more efficient aircraft have driven the introduction of carbon-epoxy structure, carbon-epoxy skins, and aramid fiber-epoxy skins in civil aircraft. Aluminum may be a good EM shield against HIRF and hence electronic circuits which are provided inherent protection. However, some

composites are poor EM shields, causing HIRF to irradiate the electronic systems on such aircraft with relatively little attenuation. So electromagnetic shielding is an important technique in electromagnetic compatibility (EMC). It can restrain electromagnetic energy radiation and prevent the electromagnetic interference effectively.

Metallic shielding enclosures are frequently employed to protect against radiation from both external EM fields and electromagnetic leakage from interior components. However, the integrity of these enclosures is often compromised by apertures of various sizes and shapes used to accommodate visibility, ventilation or access to interior components, such as input and output connections, control panels, visual-access windows, ventilation panels, etc. Since these apertures at appropriate electromagnetic frequencies behave as very efficient antennas, they also become sources of electromagnetic interference problems for both EM emission and susceptibility.

So it is very important to know the EM shielding effectiveness of shielding enclosures in the presence of these apertures. The EM shielding effectiveness study may also help in locating these apertures at proper places to reduce the EM emission or improving the immunity of electronic components present inside the metallic enclosure.

Nowadays the EM shielding effectiveness has becoming a hot research area.

Robinson et al. [1, 2] introduced a very simple analytical method based on transmission line model. However, this approach is limited by the assumption of thin apertures, simple geometries, negligible mutual coupling between apertures and fields can be calculated only at points in front of the aperture. In past years, some numerical techniques have been applied to the analysis of shielding effectiveness, such as finite difference time domain (FDTD) [3, 4] finite element method (FEM) [5, 6] method of moments (MoM) [7, 8] transmission line matrix (TLM) [9, 10] and hybrid method[11] are utilised with good accuracy over a broad frequency band at the cost of large amount of computer memory and CPU time. Deshpande introduced a moment method technique(modal MoM) using entire domain basis functions to represent apertures fields and therefore the magnetic currents on the apertures, which can evaluate the SE of a zero thickness enclosure exposed to a normally incident plane wave accurately at the center inside enclosure[12].

In this paper the modal MoM solution is formulated and by employing the surface equivalence principle and boundary conditions at each end of the aperture. The shielding effectiveness of enclosure with different shapes apertures are calculated at many other points inside the cavity. A very good agreement among the results of the proposed technique, results available in the literature and experimental results is observed.

2. ELECTROMAGNETIC PROBLEM

The shielding effectiveness of an enclosure is defined as

$$E\text{-shielding (dB)} = -20 \log \left(\frac{|E_{int}|}{|E_{ext}|} \right) \quad (1)$$

Where E_{int} is the electric field at a given point inside the enclosure and E_{ext} is the field at the same point in the absence of the enclosure. Therefore, the problem of estimation of shielding effectiveness is

$$E_{apt}(z=0) = \sum_{r=1}^R \left[\begin{aligned} & \hat{y} \sum_p \sum_q U_{rpq} \sin \left(\frac{p\pi}{L_r} \left(\frac{L_r}{2} + x - x_{cr} \right) \right) \times \cos \left(\frac{q\pi}{W_r} \left(\frac{W_r}{2} + y - y_{cr} \right) \right) \\ & + \hat{x} \sum_p \sum_q V_{rpq} \cos \left(\frac{p\pi}{L_r} \left(\frac{L_r}{2} + x - x_{cr} \right) \right) \times \sin \left(\frac{q\pi}{W_r} \left(\frac{W_r}{2} + y - y_{cr} \right) \right) \end{aligned} \right] \quad (3)$$

Where U_{rpq} and V_{rpq} are the unknown amplitudes of the pq th mode of magnetic current on the outer of the r th aperture, $U_{rpq} \neq 0$ and $V_{rpq} \neq 0$ for

essentially the problem of calculating the cavity fields excited by a plane wave incident from free space upon the shielding enclosure.

Figure 1 shows a rectangular enclosure with rectangular apertures exposed to a normal incident plane wave. The dimensions of the cavity are $a \times b \times c$. There are r number of apertures and the dimensions of the r th aperture are $L_r \times W_r$. The orientation of the reference axes is also shown with the origin at the lower right corner of the front wall.

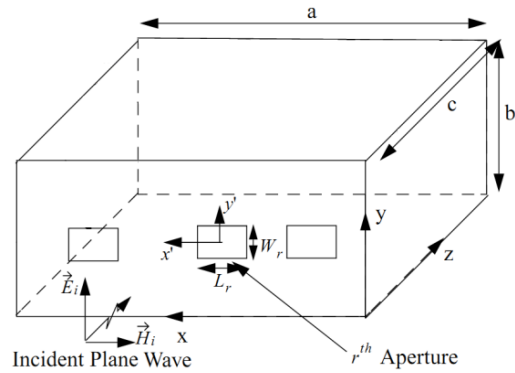


Figure 1. Geometry Of Rectangular Enclosure With Rectangular Apertures Exposed To A Normal Incident Plane Wave

2.1. Apertures Fields And Equivalent Magnetic Currents

In the modal MoM formulation, we assume that the apertures are relatively small compared to the walls in which they are located and are placed far enough away from the edges of the enclosure. In addition, the edge diffracted fields are neglected. These assumptions enable us to use image theory and equivalence principles, using the surface equivalence principle, the apertures both internal and external to the enclosure can be replaced by equivalent magnetic currents of

$$M = n \times E_{apt} \quad (2)$$

Where E_{apt} is the aperture electric field and n is the aperture normal vector.

$$x_{cr} - \frac{L_r}{2} \leq x \leq x_{cr} + \frac{L_r}{2}, \quad y_{cr} - \frac{W_r}{2} \leq y \leq y_{cr} + \frac{W_r}{2}, \quad \text{and } U_{rpq} = V_{rpq} = 0 \text{ otherwise.}$$



L_r and W_r are the length and width of r th aperture, x_{cr} and y_{cr} are center coordinates of the r th aperture. \hat{x} , \hat{y} are the unit vectors in x , y directions.

The unknown amplitudes U_{rpq} and V_{rpq} are determined by setting up coupled integral equations.

Using the equivalence principle, the equivalent magnetic currents are

$$M_{apt} = n_1 \times E_{apt} = -\hat{z} \times E_{apt}(z=0) \\ = \sum_{r=1}^R [\hat{x} \sum_p \sum_q U_{rpq} \Psi_r - \hat{y} \sum_p \sum_q V_{rpq} \Phi_r] \quad (4) \\ = \sum_{r=1}^R M_{r1}$$

Where

$$\Psi_r = \sin \left(\frac{p\pi}{L_r} \left(\frac{L_r}{2} + x - x_{cr} \right) \right) \times \cos \left(\frac{q\pi}{W_r} \left(\frac{W_r}{2} + y - y_{cr} \right) \right) \quad (5)$$

$$\Phi_r = \cos \left(\frac{p\pi}{L_r} \left(\frac{L_r}{2} + x - x_{cr} \right) \right) \times \sin \left(\frac{q\pi}{W_r} \left(\frac{W_r}{2} + y - y_{cr} \right) \right) \quad (6)$$

$$E_x^I = \sum_{r=1}^R \sum_p \sum_q \frac{-V_{rpq}}{4\pi^2} \int_{-\infty}^{\infty} \int_{-\infty}^{\infty} e^{-jk_z|z-z'|} \phi_{rpqy} e^{jk_x x + jk_y y} dk_x dk_y \quad (10)$$

$$E_y^I = \sum_{r=1}^R \sum_p \sum_q \frac{-U_{rpq}}{4\pi^2} \int_{-\infty}^{\infty} \int_{-\infty}^{\infty} e^{-jk_z|z-z'|} \psi_{rpqy} e^{jk_x x + jk_y y} dk_x dk_y \quad (11)$$

$$E_z^I = \sum_{r=1}^R \sum_p \sum_q \frac{-1}{4\pi^2} \int_{-\infty}^{\infty} \int_{-\infty}^{\infty} e^{-jk_z|z-z'|} \frac{V_{rpq} \phi_{rpqy} k_x + U_{rpq} \psi_{rpqy} k_y}{k_z} e^{jk_x x + jk_y y} dk_x dk_y \quad (12)$$

In expressions (10)-(12) ϕ_{rpqy} is the Fourier transform of Φ_{rpqy} and ψ_{rpqy} is the Fourier transform of Ψ_{rpqy} .

2.3. Electromagnetic Field inside Enclosure

The equivalent magnetic currents, present on the apertures of the enclosure, radiate electromagnetic

$$H_x^{IIx0} = \frac{-j\omega}{k_0^2} \sum_{r=1}^R \sum_{p,q} U_{rpq} \sum_{m,n} \frac{-\epsilon_0}{k_1} \frac{\epsilon_{0m}\epsilon_{0n}}{ab \sin(k_1 c)} \left(k_0^2 - \left(\frac{m\pi}{a} \right)^2 \right) \times \sin \left(\frac{m\pi x}{a} \right) \cos \left(\frac{n\pi y}{b} \right) \cos(k_1(z-c)) I_{rpqmnx} \quad (13)$$

$$H_y^{IIx0} = \frac{-j\omega}{k_0^2} \sum_{r=1}^R \sum_{p,q} U_{rpq} \sum_{m,n} \frac{-\epsilon_0}{k_1} \frac{\epsilon_{0m}\epsilon_{0n}}{ab \sin(k_1 c)} \frac{m\pi}{a} \left(-\frac{n\pi}{b} \right) \times \cos \left(\frac{m\pi x}{a} \right) \sin \left(\frac{n\pi y}{b} \right) \cos(k_1(z-c)) I_{rpqmnx} \quad (14)$$

$$H_z^{IIx0} = \frac{-j\omega}{k_0^2} \sum_{r=1}^R \sum_{p,q} U_{rpq} \sum_{m,n} \frac{-\epsilon_0}{k_1} \frac{\epsilon_{0m}\epsilon_{0n}}{ab \sin(k_1 c)} \frac{m\pi}{a} (-k_1) \times \cos \left(\frac{m\pi x}{a} \right) \cos \left(\frac{n\pi y}{b} \right) \sin(k_1(z-c)) I_{rpqmnx} \quad (15)$$

In (13)-(15),

2.2. Electromagnetic Field Outside Enclosure

Consider the aperture on the $z=0$ plane, the scattered EM field outside due to the r th aperture can be determined by solving electric vector potential

$$E = -\frac{1}{\epsilon_0} \nabla \times F \quad (7)$$

$$H = -\frac{j\omega}{k_0^2} (k_0^2 F + \nabla \nabla \cdot F) \quad (8)$$

Where the electric vector potential F is given by

$$F = \frac{\epsilon_0}{4\pi} \iint_{apt} 2M_r \frac{e^{-jk_0|r-r'|}}{r-r'} ds \quad (9)$$

Superposition of the scattered electromagnetic field due to all apertures on the $z=0$ plane gives the total scattered field as [12]

fields inside the enclosure. The total electromagnetic field at any point inside enclosure is obtained by a superposition of fields due to each equivalent magnetic current source. considering the x - component of the magnetic current and using dyadic Green's function, The total magnetic field inside the enclosure is then obtained from [12] as

$$I_{rpqmnx} = \sin \left(\frac{m\pi x}{a} \right) \times \cos \left(\frac{n\pi y}{b} \right) dx' dy'$$



Likewise, considering the y-component of the magnetic current and using the proper boundary conditions, The total magnetic field inside the enclosure is then obtained from [12] as

$$H_x^{Ily0} = \frac{j\omega}{k_0^2} \sum_{r=1}^R \sum_{p,q} -V_{rpq} \sum_{m,n} \frac{-\epsilon_0 - \epsilon_{0m}\epsilon_{0n}}{k_l ab \sin(k_l c)} \left(-\frac{m\pi}{a}\right) \frac{n\pi}{b} \times \sin\left(\frac{m\pi x}{a}\right) \cos\left(\frac{n\pi y}{b}\right) \cos(k_l(z-c)) I_{rpqmny} \quad (16)$$

$$H_y^{Ily0} = \frac{j\omega}{k_0^2} \sum_{r=1}^R \sum_{p,q} -V_{rpq} \sum_{m,n} \frac{-\epsilon_0 - \epsilon_{0m}\epsilon_{0n}}{k_l ab \sin(k_l c)} \left(k_0^2 - \left(\frac{n\pi}{b}\right)^2\right) \times \cos\left(\frac{m\pi x}{a}\right) \sin\left(\frac{n\pi y}{b}\right) \cos(k_l(z-c)) I_{rpqmny} \quad (17)$$

$$H_z^{Ily0} = \frac{j\omega}{k_0^2} \sum_{r=1}^R \sum_{p,q} -V_{rpq} \sum_{m,n} \frac{-\epsilon_0 - \epsilon_{0m}\epsilon_{0n}}{k_l ab \sin(k_l c)} \frac{n\pi}{b} (-k_l) \times \cos\left(\frac{m\pi x}{a}\right) \cos\left(\frac{n\pi y}{b}\right) \sin(k_l(z-c)) I_{rpqmny} \quad (18)$$

In (16)-(18), $H_x^{II} = H_x^{IIx0} + H_x^{Ily0} \quad (19)$

$$I_{rpqmny} = \iint_q \Phi_{rpqy}(x',y') \cos\left(\frac{m\pi x'}{a}\right) \sin\left(\frac{n\pi y'}{b}\right) dx' dy' \quad H_y^{II} = H_y^{IIx0} + H_y^{Ily0} \quad (20)$$

For a unique solution the electromagnetic fields in various regions satisfy continuity conditions over their common surfaces. The tangential electric fields over the apertures are continuous. The tangential magnetic over the apertures also must be continuous, thus yielding coupled integral equations with the magnetic currents as known variables. The coupled integral equation in conjunction with the method of moments can be solved for the amplitudes of magnetic currents.

Applying the continuity of tangential magnetic field on the z = 0 plane yields

$$H_x^I|_{z=0} + H_{xi}|_{z=0} = H_x^{II}|_{z=0} \quad (21)$$

$$H_y^I|_{z=0} + H_{yi}|_{z=0} = H_y^{II}|_{z=0} \quad (22)$$

Now selecting $\Psi_{r'p'q'x}$ as a testing function and use of Galerkin's method reduces the (21) to

$$I_{r'p'q'xi} = \sum_{r=1}^R \sum_{p,q} (U_{rpq} Y_{rpqr'p'q'}^{x1x1} + V_{rpq} Y_{rpqr'p'q'}^{x1y1}) \quad (23)$$

Where

2.4. Derivation of Integral Equation

The total tangential fields inside the cavity from apertures are written as

$$Y_{rpqr'p'q'}^{x1x1} = \frac{-j\omega}{k_0^2} \sum_{m,n=0}^{\infty} \frac{-\epsilon_0 - \epsilon_{0m}\epsilon_{0n}}{k_l ab \sin(k_l c)} \left(k_0^2 - \left(\frac{m\pi}{a}\right)^2\right) \cos(k_l c) I_{rpqmnx} I_{r'p'q'mnx} + \frac{\omega\epsilon_0}{4\pi^2 k_0^2} \int_{-\infty}^{+\infty} \int_{-\infty}^{+\infty} \Psi_{rpqx} \Psi_{r'p'q'x}^* \frac{k_0^2 - k_x^2}{k_z} dk_x dk_y \quad (24)$$

$$Y_{rpqr'p'q'}^{x1y1} = \frac{j\omega}{k_0^2} \sum_{m,n=0}^{\infty} \frac{-\epsilon_0 - \epsilon_{0m}\epsilon_{0n}}{k_l ab \sin(k_l c)} \left(-\frac{m\pi}{a}\right) \left(\frac{n\pi}{b}\right) \cos(k_l c) I_{rpqmny} I_{r'p'q'mnx} + \frac{\omega\epsilon_0}{4\pi^2 k_0^2} \int_{-\infty}^{+\infty} \int_{-\infty}^{+\infty} \Phi_{rpqy} \Psi_{r'p'q'x}^* \frac{-k_x k_y}{k_z} dk_x dk_y \quad (25)$$

$$I_{r'p'q'xi} = \iint_{r'p'q'} H_{xi} \Psi_{r'p'q'x} dx dy \quad (26) \quad I_{r'p'q'yi} = \sum_{r=1}^R \sum_{p,q} (U_{rpq} Y_{rpqr'p'q'}^{y1x1} + V_{rpq} Y_{rpqr'p'q'}^{y1y1}) \quad (27)$$

Similarly, selecting $-\Phi_{r'p'q'y}$ as a testing function and use of Galerkin's method reduces the (22) to

Where

$$Y_{rpqr'p'q'}^{y1x1} = \frac{j\omega}{k_0^2} \sum_{m,n=0}^{\infty} \frac{-\epsilon_0 - \epsilon_{0m}\epsilon_{0n}}{k_l ab \sin(k_l c)} \left(\frac{m\pi}{a}\right) \left(-\frac{n\pi}{b}\right) \cos(k_l c) I_{rpqmnx} I_{r'p'q'mny} + \frac{\omega\epsilon_0}{4\pi^2 k_0^2} \int_{-\infty}^{+\infty} \int_{-\infty}^{+\infty} \Psi_{rpqx} \Phi_{r'p'q'y}^* \frac{-k_x k_y}{k_z} dk_x dk_y \quad (28)$$

$$Y_{rpqr'p'q'}^{y1y1} = -\frac{j\omega}{k_0^2} \sum_{m,n=0}^{\infty} \frac{-\epsilon_0 - \epsilon_{0m}\epsilon_{0n}}{k_l ab \sin(k_l c)} \left(k_0^2 - \left(\frac{n\pi}{b}\right)^2\right) \cos(k_l c) I_{rpqmny} I_{r'p'q'mny} - \frac{\omega\epsilon_0}{4\pi^2 k_0^2} \int_{-\infty}^{+\infty} \int_{-\infty}^{+\infty} \Phi_{rpqy} \Phi_{r'p'q'y}^* \frac{(k_0^2 - k_x^2)}{k_z} dk_x dk_y \quad (29)$$

$$I_{r'p'q'yi} = \iint_{r'p'q'} H_{yi} \Phi_{r'p'q'x} dx dy \quad (30)$$

Equation (23) and (27) can be written in a matrix form as

$$\begin{bmatrix} Y_{rpqr'p'q'}^{x1x1} & Y_{rpqr'p'q'}^{x1y1} \\ Y_{rpqr'p'q'}^{y1x1} & Y_{rpqr'p'q'}^{y1y1} \end{bmatrix} \begin{bmatrix} U_{rpq} \\ V_{rpq} \end{bmatrix} = \begin{bmatrix} I_{r'p'q'xi} \\ 0 \end{bmatrix} \quad (31)$$

For normal incidence

$$I_{r'p'q'xi} = \begin{cases} H_{xi} W_r \left(\frac{1 - \cos(p'\pi)}{p'\pi/L_{r'}} \right), & \text{for}(q' = 0) \\ 0, & \text{for}(q' \neq 0) \end{cases}$$

Using the orthogonality of expansion functions it can be shown $Y_{rpqr'p'q'}^{y1x1} = Y_{rpqr'p'q'}^{x1y1} = 0$, hence equation (31) simplifies to

$$[Y_{rpqr'p'q'}^{x1x1}] [U_{rpq}] = [I_{r'p'q'xi}] \quad (32)$$

The matrix equation (32) can be numerically solved for the unknown amplitudes of equivalent magnetic currents induced on the apertures due to given incident field. From the knowledge of these amplitudes electromagnetic field inside as well as outside the enclosure can be obtained.

3. VALIDATION OF THE PRESENT TECHNIQUE

In this section, we consider a rectangular enclosure of size (30cm × 12cm × 30cm) with a rectangular aperture of size (10cm × 0.5cm) located at the center of the front wall (15cm, 6cm, 0) for the validation of the present technique, as illustrated in Figure 2. The enclosure is illuminated by a normal incident plane wave at 0 polarization.

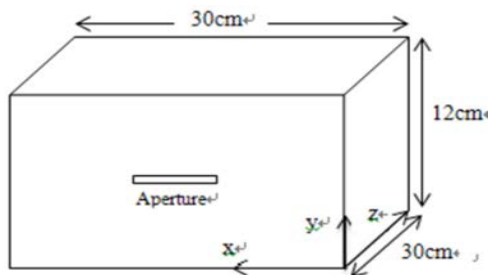


Figure 2. Geometry Of 30cm×12cm×30cm Enclosure With A Single Aperture At (15cm, 6cm, 0)

Assuming only expansion mode on the aperture and considering only dominant mode inside the cavity. The shielding effectiveness is calculated at the center of the cavity. Electric field shielding

obtained using expression (32) is plotted in Figure 3 along with the results from [2]. It is observed that the numerical data obtained using the present method agrees well with the earlier published results. Experimental data from [2] is also reproduced in Figure 3.

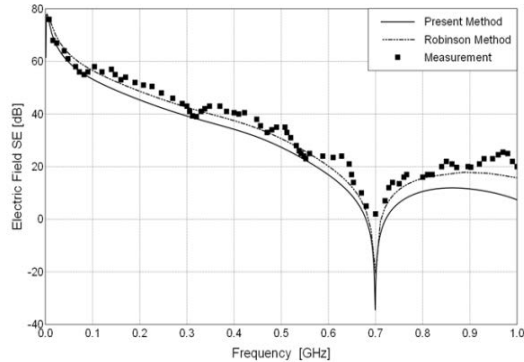


Figure 3. Electric field Shielding At The Center Of 30cm×12cm×30cm Enclosure 10cm×0.5cm Aperture Located At 15cm×6cm In Z=0 Plane With Dominant Cavity Mode Considered.

4. RESULTS AND DISCUSSION

In this section, in order to study the electric field shielding of different points in the cavity, the same geometry with Figure 2 is selected. The enclosure is illuminated by a normal incident plane wave at 0 polarization. The shielding effectiveness with dominant cavity mode considered is also calculated at many different points in the cavity.

Shielding effectiveness at five different plane inside the enclosure obtained using the present method are plotted in Figure 4 which discusses electric field shielding effectiveness versus different x value. From the numerical data presented in Figure 4, it may be observed that electric field SE below the resonance frequency is influenced heavily by x value. The maximum and minimum of electric field SE occur at z=250mm and z=50mm respectively. The maximum difference of electric field SE is almost 20dB in Figure 4(c). Figure 4(c) also shows that the electric field SE increases rapidly to more than 60dB from 3dB at 0.75GHz on the z=50 plane. From what has been discussed above, it can be concluded that electric field SE is lower at the points near to the apertures than at larger distance from them, but when frequency exceed the resonance frequency, this result is wrong. Therefore low frequency sensitive apparatus

inside the enclosure should be placed at the points far away from the apertures, which can improve the ability of electromagnetic compatibility.

10.0cm×0.5cm aperture to 2.23cm×2.23cm aperture and electric field SE have a rapid increase up to about 50dB at 0.75GHz at z=50mm because of modal structure of the fields. Figure.5 confirms the electric field SE dependence upon distance from the apertures. We also note that the apertures with different shape but same area have different effect on electric field SE. For one aperture case, from discussed above, we can conclude that square aperture have higher electric field SE than rectangular aperture when their area is same.

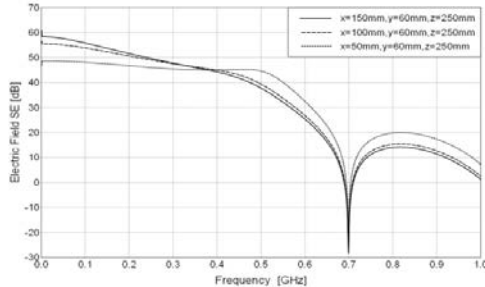


Figure 4. (A)

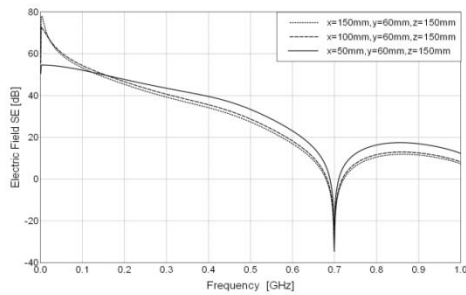


Figure 4. (B)

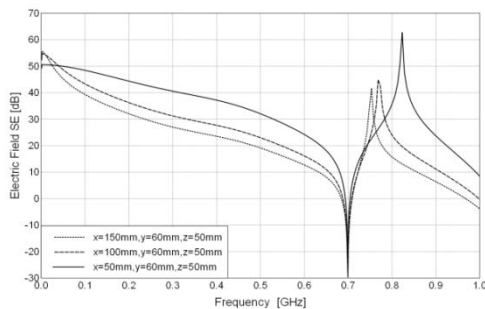


Figure 4. (C)

Figure 4. Electric field SE Versus X Value At Different Plane Of 30cm×12cm×30cm Enclosure With 10cm×0.5cm Aperture Located At 15cm×6cm In Z=0 Plane.

In this section, we discuss electric field SE results calculated at three different points versus different shapes apertures. We also consider a 30 cm × 12cm × 30cm enclosure with rectangular aperture of size (10 cm × 0.5cm, 5.0 cm × 1.0cm and 2.23cm × 2.23cm) located at the center of the front wall (15cm, 6cm, 0) respectively. The enclosure is illuminated by a normal incident plane wave at 0 polarization.

Figure.5 (a), (b) and (c) presents three plots of electric field SE versus three different shapes aperture with same area respectively. We observe a similar changed trend in Figure.5 (a), (b) and (c) that all the resonance frequency is about 0.7 GHz, electric field SE increase in turn from

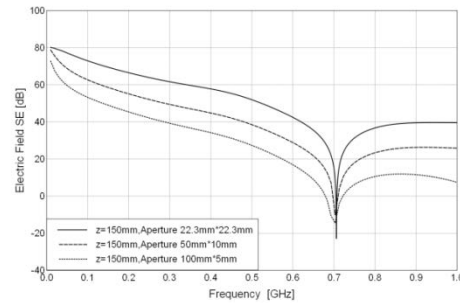


Figure 5(A) Electric field SE Calculated At Z=150mm, X=150mm, Y=60mm

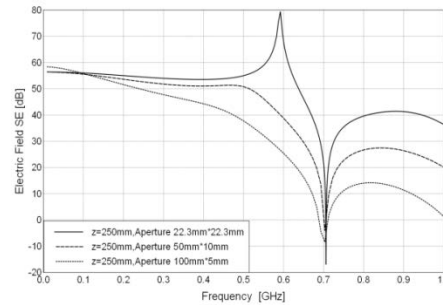


Figure 5(B) Electric field SE Calculated At Z=250mm, X=150mm, Y=60mm

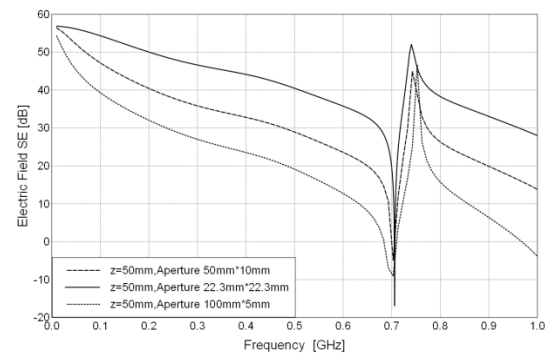


Figure 5(C) Electric field SE Calculated At Z=50mm, X=150mm, Y=60mm

Figure 5. Electric field SE Calculated At Different Points Inside 30cm×12cm×30cm Enclosure With A Aperture Of Size (10cm×0.5cm, 5.0cm×1.0cm And 2.23cm×2.23cm)



5. CONCLUSION

In this paper, the influence of the calculation point of SE and apertures' shape on electromagnetic shielding effectiveness has been investigated. The modal MoM solution is formulated, and by employing the surface equivalence principle and boundary conditions at each end of the aperture, the problem is solved. Simulation results are well agreed with data available in the literature. The results of the present analysis show that lower electric field SE near the aperture than at location inside the enclosure farther away from the aperture, the electric field SE is also seriously affected by aperture shape. These useful results gained in this paper have the important practical significance to improv the electric field shielding effectiveness of shielding cavity.

REFERENCES

- [1] M.P. Robinson, J.D. Turner, D.W.P. Thomas, Etc. Shielding effectiveness of a rectangular enclosure with a rectangular aperture. *Electron. Lett.* 1996; 32(17):1559-1560.
- [2] M.P. Robinson, T.M. Benson, C. Christopoulos, Etc. Analytical formulation for the shielding effectiveness of enclosures with apertures. *IEEE Transactions on Electromagn Compatibility.* 1998; 40(3): 240–248.
- [3] LIM., NUBEL J., DREWNIAK J.L, Etc. EMI from cavity modes of shielding enclosures – FDTD modeling and measurements. *IEEE Transactions on Electromagn Compatibility.* 2000; 42(1):29–38.
- [4] M. Li, J. Nuebel, J. L. Drewniak, T. H. Hubing, Etc. EMI from cavity modes of shielding enclosures—FDTD modeling and measurements. *IEEE Transactions on Electromagn Compatibility.* 2000; 42(1): 29–38.
- [5] BENHASSINE S., PICHON L., TABBARA W. An efficient finite-element time-domain method for the analysis of the coupling between wave and shielded enclosure. *IEEE Transactions on Magnetics.* 2002; 38(2): 709–712.
- [6] W. P. Carpes Jr., L. Pinchon, and A. Razeq. Analysis of the coupling of an incident wave with a wire inside a cavity using an FEM in frequency and time domains. *IEEE Transactions on Electromagn Compatibility.* 2002; 44(3): 470–475.
- [7] WALLYN W., DE ZUTTER D., ROGIER H. Prediction of the shielding and resonant behavior of multisection enclosures based on magnetic current modeling. *IEEE Trans. IEEE Transactions on Electromagn Compatibility.* 2002; 44 (1):130–138.
- [8] G. Wu, X.-G. Zhang, Z.-Q. Song, and B. Liu . Analysis on Shielding Performance of Metallic Rectangular Cascaded Enclosure with Apertures. *Progress In Electromagnetics Research Letters.* 2011; 20: 185-195.
- [9] PODLOZNY V., CHRISTOPOULOS C., PAUL J. Efficient description of fine features using digital filters in time domain computational electromagnetics. *IET Sci. Meas. Technol.*,2002, 149(5): 254–257.
- [10] R. Attari , K. Barkeshli. Application of the transmission line matrix method to the calculation of the shielding effectiveness for metallic enclosures. in *Proc. IEEE Antennas Propagation Soc. Int. Symp. Texas.* 2002: 302–305.
- [11] Wu,G.Zhang,X.G.;Liu,B. A Hybrid Method for Predicting the Shielding Effectiveness of Rectangular Metallic Enclosures with Thickness Apertures. *Journal of Electromagnetic Waves and Applications.* 2010; 24(8):1157-1169.
- [12] Electromagnetic field penetration studies (NASA/CR-2000-210 297),M. D. Deshpande. (2000, Jun.).[Online]. Available: http://techreports.larc.nasa.gov/ltrs/PDF/2000/cr/NASA-2000-cr210_297.pdf.